

Adsorption of Phenylacetylene on Si(100)-2 × 1: Kinetics and Structure of the Adlayer

Olivier Pluchery,* Romain Coustel, Nadine Witkowski, and Yves Borensztein

Institut des Nanosciences de Paris, UMR-CNRS 7688, Universités Paris VI and Paris VII, Campus Boucicaut, 140 rue de Lourmel, 75015 Paris, France

Received: June 26, 2006; In Final Form: September 18, 2006

Direct adsorption of phenylacetylene on clean silicon surface Si(100)-2 × 1 is studied in ultrahigh vacuum (UHV). The combination of scanning tunnel microscopy (STM) and surface differential reflectance spectroscopy (SDRS) with Monte Carlo calculations are put together to draw a realistic kinetic model of the evolution of the surface coverage as a function of the molecular exposure. STM images of weakly covered surfaces provide evidence of two very distinct adsorption geometries for phenylacetylene, with slightly different initial sticking probabilities. One configuration is detected with STM as a bright spot that occupies two dangling bonds of a single dimer, whereas the other configuration occupies three dangling bonds of adjacent dimers. These data are used to implement a Monte Carlo model which further serves to design an accurate kinetic model. The resulting evolution toward saturation is compared to the optical data from surface differential reflectance spectroscopy (SDRS). SDRS is an in situ technique that monitors the exact proportion of affected adsorption sites and therefore gives access to the surface coverage which is evaluated at 0.65. We investigate the effect of surface temperature on this adsorption mechanism and show that it has no major effect either on kinetics or on structure, unless it passes the threshold of dissociation measured at ca. 200 °C. This offers a comprehensive image of the whole adsorption process of phenylacetylene from initial up to complete saturation.

I. Introduction

Controlling and monitoring the adsorption of small organic molecules on silicon substrates is the center of sustained efforts of many research groups nowadays. This research is of fundamental interest and simultaneously anticipates the need of the electronic industry that is attempting to connect molecular electronic functions (bistable molecules, memories, conductive organic layer) to CMOS (complementary metal oxide semiconductor) devices and build new sensors. The challenge is therefore to fabricate ultrathin films of the monolayer size that exhibit uniform and reproducible properties. The use of molecular materials to build films has already proven its relevance because the electronic systems of conjugated molecules add to the film very promising electronic properties: high charge mobility, switching behavior, anisotropic conductivity (molecular nanowires), and nonlinear response.¹ In an ultrahigh vacuum environment, Si(100) silicon surface exhibits a 2 × 1 reconstruction after a suitable preparation. From a morphological point of view, this surface is made of rows of dimers that could be seen as an efficient template to direct the self-organization of molecules upon adsorption.² From a chemical point of view, the bond between two silicon atoms of one dimer has similarities with a π bond and gives rise to cycloadditions.³ The direct adsorption of a large range of molecules, such as acetylene,⁴ benzene,^{5–7} and biphenyl⁸ has been largely investigated in the past decade so that the reactivity of some functional groups on this surface is beginning to be known.

The challenge is to succeed in building an ordered organic monolayer and to simultaneously preserve a functional group that would make further reactions possible or at least preserve electronic conjugation. Moreover, if the adsorbed layer still has unsaturated bonds or conjugated π electrons systems, it could

exhibit interesting electronic properties such as charge-transfer capability⁹ or fluorescence.¹⁰

In that respect, phenylacetylene (PA) is an interesting molecule that has received little attention so far. PA has two chemically active sites: one is the acetylene triple bond and the second one is the benzene ring with its π electrons system (see Figure 1a). This offers a priori two adsorption configurations depending on which one of the two functional groups reacts with the silicon dimers. The adsorption of PA on Si(111)-7 × 7 has been investigated with simulations, and it was concluded that adsorption occurs through the acetylene group only.¹¹ However, a comparison with the reactivity of PA on the Si(100)-2 × 1 surface is not straightforward. Actually, scanning tunnel microscopy (STM) observations have been carried out in ultrahigh vacuum (UHV) and at room temperature, after deposition of a small amount of PA on Si(100)-2 × 1. They are combined with calculations and show that two types of adsorbed species are detected on the surface.¹² But, the case of the saturated surface is not considered. Moreover, these results apparently stand in contradiction to another study where high-resolution electron energy loss spectroscopy (HREELS) and X-ray photoelectron spectroscopy (XPS) were used to monitor the deposition of PA at low temperature (110 K).¹³ The conclusion was that PA adsorbs with a single configuration through the acetylene group. This would suggest that temperature plays a decisive role in sorting out the possible adsorption configurations. Therefore, this is one scope of the present paper to question whether temperature is the relevant kinetic parameter that may serve as a “handle” to orient the reactivity of PA on Si(100)-2 × 1 toward a single adsorption geometry. Temperatures ranging from room temperature up to that for the dissociation of PA will be investigated.

Moreover, the two π electrons systems of PA are conjugated so that the π electrons from the phenyl ring are delocalized

* Corresponding author. olivier.pluchery@insp.jussieu.fr. Tel.: +33 144 27 94 10. Fax: +33 1 44 27 39 82.

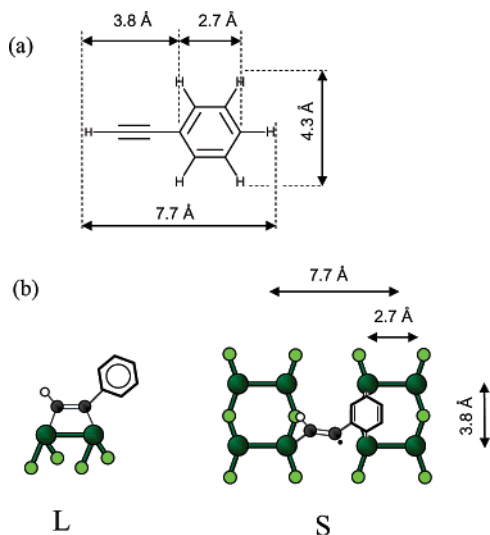


Figure 1. Phenylacetylene molecule (a) and its two possible geometries of adsorption on Si(100)-2 \times 1 (b) corresponding to the large (L) and small (S) protrusions observed with STM.

until the end of the acetylene triple bond. In case of an adsorption controlled by a cycloaddition through the acetylene group, this conjugation would remain. If the resulting PA monolayer is self-organized, it would certainly exhibit interesting properties such as long range electronic delocalization. Actually, PA has been used to build a monolayer on hydrogenated silicon^{14,15} and the electronic properties of the PA monolayer were investigated by mean of kelvin probe force microscopy (KPFM). A strong enhancement of the conductivity has been evidenced.¹⁵ Although the adsorption mechanisms were different from our case, these results support the interest for studying this molecule.

In this article, we use room-temperature STM to gain information on the adsorbed PA on Si(100)-2 \times 1 at low coverage. For saturation coverage, UV-visible optical differential spectroscopy gives access to the exact coverage as well as to the kinetics of the surface reaction. We analyze the optical data taken at different temperatures with the help of a Monte Carlo model and conclude that PA always adsorbs with two simultaneous configurations as long as the surface temperature does not exceed 200 °C which corresponds to the dissociation of PA. Apparently, the kinetics of the reaction is not strongly sensitive to temperature within the range we have considered: from room temperature up to 320 °C.

II. Experiments

Our experiments are carried out in two interconnected ultrahigh vacuum chambers with a base pressure of 5×10^{-11} torr. The preparation chamber is equipped with conventional analysis techniques such as low-energy electron diffraction (LEED), Auger spectroscopy (OMICRON), and a quadrupole mass spectrometer (PFEIFFER Prisma) used to check the purity of the molecules and calculate the integrated amount of PA introduced into the chamber. The total pressure P is measured with Bayart-Alpert ionization gauge, calibrated to N₂. The actual pressure, defined according to the kinetic theory of gases, could be obtained by dividing the displayed pressure by a correction factor evaluated around 6.0 ± 0.2 for a molecule like PA.¹⁶ However, an accurate calculation should take into account the geometry of the chamber and the characteristics of the molecular beam. This is not useful for interpreting our data, and consequently in this paper, we are using the “uncorrected

exposure” x calculated the following way: $dx = P \times dt$. The gauge is situated at 40 cm from the leak valve used to introduce the gases, whereas the sample is at 15 cm. In this paper, we use an optical technique called surface differential reflectance spectroscopy (SDRS) to characterize the modifications of the surface. It monitors the relative change of the reflectivity of the surface due to molecular adsorption. SDRS spectra presented in our work display the quantity $\Delta R/R = (R_{\text{clean}} - R_{\text{ads}}(\theta))/R_{\text{clean}}$ as a function of the photon energy E expressed in eV. $R_{\text{ads}}(\theta)$ is the reflectivity of the surface for a given coverage of the studied molecule, and R_{clean} is the reflectivity of the clean surface prior to adsorption. This technique probes the surface states of silicon and turns out to be highly sensitive to the saturation of the dangling bonds, almost independently of the nature of the molecules.¹⁷ This is a handful method to access the exact covering rate of the surface. Simultaneously, it offers an elegant way to check whether the dimers are broken as well.¹⁸ These features of SDRS will be developed further on.

The scanning tunnel microscope is in the second UHV chamber. This is a commercial STM-AFM instrument from OMICRON working at room temperature. The tungsten tips are prepared by chemical etching (solution of 2 M KOH) and then resistively heated in the preparation chamber to remove the tungsten oxide layer. The sample are cut from a Si(100) n -type wafer (phosphorus doped, SILTRONIX) with 1–10 $\Omega \cdot \text{cm}$ resistivity and a miscut less than 0.05°. They are mounted into the sample holder carefully avoiding any contact with steel tools or any Ni-containing tools in order to avoid surface contamination. This would show up in the STM images as linearly organized depressions perpendicular to the dimer rows.^{19,20} The sample preparation procedure is the following: rinsing in acetone and then ethanol with ultrasonic bath prior to mounting the sample. The sample is degassed in the UHV preparation chamber for at least 12 h at 650 °C and then *flushed* three times at 1050 °C for at least 5 s, carefully preventing the pressure from rising over 5×10^{-10} torr in order to obtain a correctly reconstructed surface. No special procedure is used to cool the sample. The crucial point to obtain an almost defect-free surface is the value of the peak pressure during the flash.²¹ To maintain a good pressure during this step, it is useful to degas the sample manipulator with a dummy sample at 1050 °C for 1 h just before the flashes. The average number of defects is estimated at 3%. The silicon sample is heated by direct current flow, and the temperature is measured with an optical pyrometer ($\epsilon = 0.66$) in the range of 300–1050 °C with an accuracy of 5 °C. For temperatures ranging from room temperature to 300 °C, the temperature is evaluated on the basis of the electrical power flowing through the sample. Phenylacetylene is purchased from SIGMA-Aldrich and purified by about 10 pump-and-thaw cycles before use. PA, being liquid at room temperature with a partial vapor pressure of 10 Torr, is introduced directly into the chamber with a leak valve. Its purity is checked with the mass spectrometer to ensure the amount of water dissolved in the liquid is negligible.

III. Results

1. Adsorption of PA at Low Coverage Monitored with STM. Phenylacetylene (PA) molecules have been adsorbed on Si(100)-2 \times 1 at various temperatures and then observed with room-temperature STM. The first experiment we report is the deposition of PA at room temperature with a pressure of 4×10^{-9} torr and a total amount of 0.08 “uncorrected” Langmuir. The corresponding STM image of the filled states is presented in Figure 2a. The image is recorded at a bias of -2.0 V and a

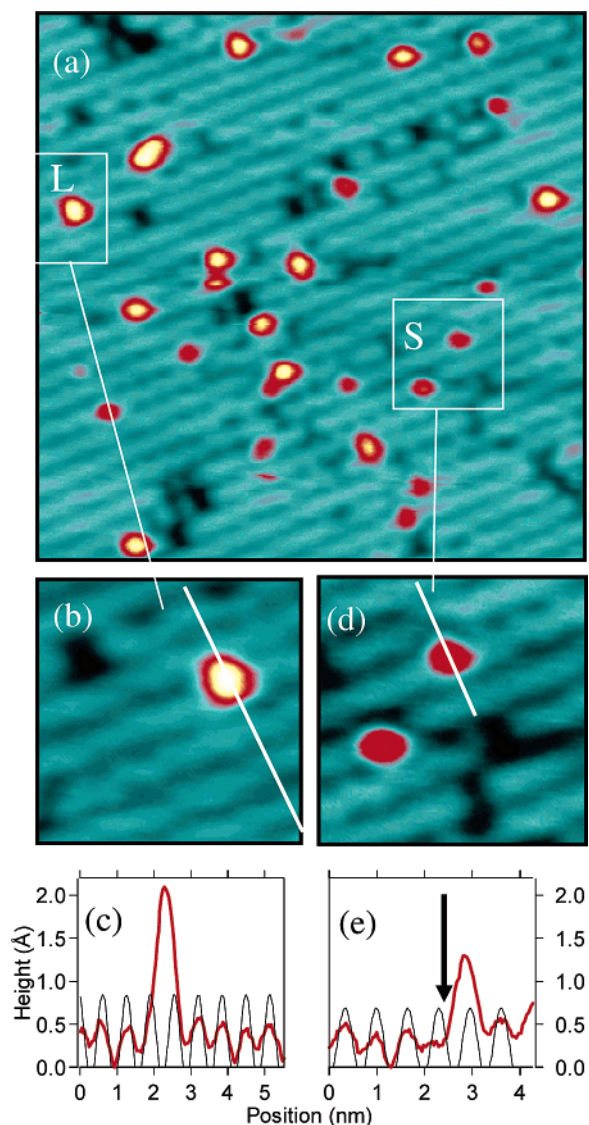


Figure 2. (a) $15 \times 15 \text{ nm}^2$ STM image of Si(100)- 2×1 after deposition of 0.08 Langmuir of phenylacetylene (PA) at room temperature (RT). Image b is a $4 \times 4 \text{ nm}^2$ scan centered on a PA molecule adsorbed in the L configuration, and the corresponding profile following the indicated line is represented in part c. Parts d and e are similar illustrations for the S species. The arrow on inset e points to the neighboring dimer which is systematically disturbed by this type of adsorption. For all STM images, tunneling conditions are -2.0 V and 0.1 nA .

tunneling current of 0.1 nA . It mainly reveals two types of spots: large and small protrusions denoted L and S, respectively, in the figure. In addition to these features, the image displays a few defects, mainly missing dimers. They show up as rectangle-shaped black depressions. The positions of the adsorbed PA molecules are independent of these defects: no special concentration of molecules was ever observed around the defects or near the steps. The inset (Figure 2b) reveals that the large spots correspond to structures of an average height of $2.1 \pm 0.1 \text{ \AA}$ and wider than a dimer row. The electronic density is asymmetric relative to the dimer row with its maximum lying between the rows. This is illustrated with Graph 2c where a profile running through an L spot and perpendicular to the dimer rows has been drawn. On this graph, the cosine oscillation highlights the position of the dimer rows and reveals the asymmetric position of the molecule. As for the small protrusions, their mean height is of $1.3 \pm 0.1 \text{ \AA}$. The molecule also adopts an asymmetric, albeit different, configuration relative

to the dimer row. Moreover, a faint depression is visible on the neighboring row, which is illustrated with the profile from Figure 2e. Such profiles drawn for S type configurations always show a peak positioned slightly off the rows and the neighboring dimer strongly affected by the molecule: the arrow of Graph 2e points to the disturbed dimer. This means that the molecule spans over two adjacent rows. From a global point of view, statistics done on large-scale images confirms the repartition of the adsorbed PA into two configurations. Over 181 molecules visible on a $43 \times 43 \text{ nm}^2$ image, 45% out of them have a mean volume of 35 \AA^3 and correspond to the L configuration, whereas the remaining 55% have a volume of 5 \AA^3 and are in the S configuration. This description agrees with previously published work done by Kang's group.¹² On the basis of STM images and with the help of density functional theory (DFT) calculations, they investigated the adsorption geometries of PA and proposed possible configurations for L and S. The L configuration is due to adsorption of PA via its acetylene group which preserves the phenyl ring. The bond created with silicon is strong with a calculated adsorption energy of 2.5 eV . The molecule is adsorbed on a single dimer, the phenyl group stretches across the rift toward the next dimer row, and the molecule resembles somehow a styrene molecule. In this case, one molecule saturates two dangling bonds. The S configuration does not have a definitive interpretation, but the three possible candidates all correspond to an adsorption via both the benzene ring and the acetylene end. The calculated adsorption energies are very different for the three candidates. Therefore, the configuration we retain in this paper is the most stable with an adsorption energy of 1.6 eV which is 0.5 eV more favorable than the two other possible geometries. The π electronic delocalization is destroyed, and the molecule is adsorbed in a "valley-bridge" configuration where three different dimers are implied and three dangling bonds are saturated. These two configurations are schematically represented in Figure 1b. These proposed geometries agree well with the STM images as confirmed by the two following statements. On the basis of bond lengths, the centroid of the benzene ring of L configuration is expected to be 2.5 \AA away from the axis of the dimer and is actually measured at 2.6 \AA in Figure 2c. For the S configuration, the middle of benzene is expected to be 1.3 \AA from the axis of the dimer and is measured at 1.1 \AA .

In the effort to prepare uniformly organized and electronically controlled surfaces, the coexistence of two adsorbed species is a serious problem. It is reasonable to slightly heat up the surface and try to alter the balance between L and S species. Figure 3a is an STM image scanned at room temperature of a Si(100)- 2×1 surface with 0.13 Langmuir of PA deposited at $100 \text{ }^\circ\text{C}$, and we notice again the same two configurations. Apparently, the coexistence of the two species exhibits a similar ratio. We further investigate the effect of temperature with $320 \text{ }^\circ\text{C}$ adsorption experiment. This time an amount of 0.18 Langmuir of PA was introduced on the surface. The corresponding image in Figure 3b offers a totally different situation compared to the previous ones with a large variety of features. It is impossible to clearly identify any L or S species. Lots of other adsorbates are present on this surface, and they are interpreted as fragments from dissociated PA. The black features that look like missing silicon dimers may originate from acetylene-like adsorbates,⁴ although the fragment produced from the dissociation of PA lacks one hydrogen atom to exactly match an acetylene molecule. The large and bright spot is an agglomeration of various fragments. This situation is not worth extensive

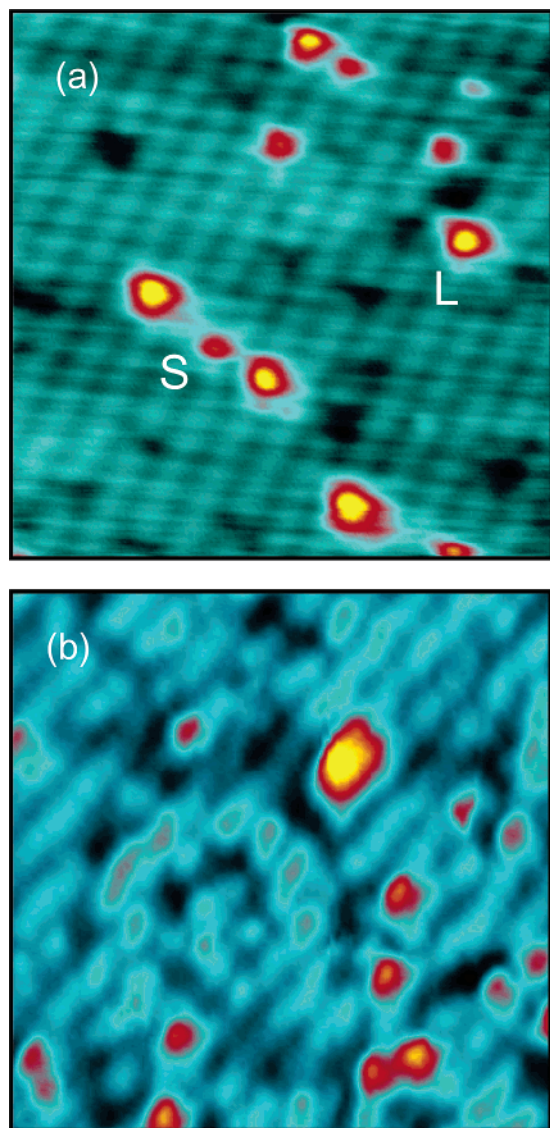


Figure 3. (a) $10 \times 10 \text{ nm}^2$ room-temperature STM images of Si(100)- 2×1 after deposition of 0.13 Langmuir of PA at 100°C (a) or 0.18 Langmuir of PA at 320°C (b). At 100°C , PA adsorbs with L and S configurations only, whereas, at 320°C , fragments of PA are also observed. Tunneling conditions are -2.0 V and 0.1 nA .

development, and it mixes the complexity of at least three species: benzene, acetylene, and phenylacetylene.

These low coverage experiments reveal that phenylacetylene adsorbs on Si(100)- 2×1 with the two configurations L and S as long as the temperature does not cause dissociation which occurs at 200°C and above. Notice that, in the case of the L configuration, the π electronic system of phenylacetylene is preserved and still spans over the entire molecule. This is definitively a central property of this adsorption geometry of PA, and it would be a major result if it were possible to saturate the silicon surface exclusively with this configuration. However, we did not succeed in imaging the saturated surface with STM at room temperature. It may be due to the nonuniformity of the surface which could be rather irregular given that the L adsorbates and S adsorbates have very different heights.

2. Adsorption of PA at Saturation Coverage Monitored with Optical Spectroscopy. The second set of experiments we report is addressing the question of saturation coverage of Si(100) with phenylacetylene. We did not obtain any satisfactory STM images of the saturated surface. Actually, the images were not reproducible and showed disorganized domains. This is

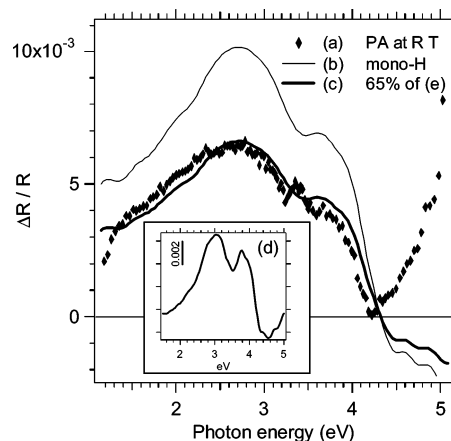


Figure 4. Surface differential reflectance spectra (SDRS) of Si(100)- 2×1 saturated surfaces with either PA at room temperature (a) or with atomic H producing the monohydride silicon surface (b). Spectrum c is obtained from spectrum b after multiplication by 0.65, indicating that 65% of the silicon dangling bonds are affected by adsorption of PA. Inset d shows the SDRS spectrum of a dihydride silicon surface with the peak at 3.8 eV indicative of the breaking of the dimers.

probably due to several factors: some molecules are sticking to the tip altering the resolution; the adsorption within two simultaneous configurations may result in a surface made of closely packed pits and bumps, and the scanning tip cannot follow this corrugation. Successful imaging of silicon saturated surfaces has been scarcely published, and this was in cases where the molecule produces a compact and organized layer.²² However, surface differential reflectance spectroscopy (SDRS) is especially adapted to monitoring the progressive saturation of the silicon surface. This technique has been described with more details elsewhere.^{23,24} SDRS is sensitive to the modification of the optical response of the silicon substrate during adsorption. The signal measured with SDRS is in the UV–visible range (1.5–5.0 eV) and mainly arises from surface states or surface modified bulk transitions. Light is shone on the surface with a 45° incidence geometry and is polarized with the electric field parallel to the surface (*s*-polarization). For Si(100)- 2×1 , it has been shown¹⁸ that the uptake of a broad peak around 2.8 eV is related to the saturation of the silicon dangling bonds. If the silicon dimers are broken, a second feature at 3.8 eV is detected, which occurs, for example, with the adsorption of atomic hydrogen at room temperature, yielding a nonreconstructed dihydride Si(100) surface (see inset d of Figure 4). Interestingly, the intensity of these features is proportional to the amount of saturated dangling bonds or broken dimers, respectively. For example, a surface whose dimers are all being saturated with atomic hydrogen exhibits a broad positive peak centered at 2.8 eV with a relative intensity increase of 1.0×10^{-2} . Note that this value is independent of the nature of the adsorbate as long as this latter does not exhibit any optical absorption around 2.8 eV. This quantitative information gained from SDRS is a unique feature of this technique, which we are going to use extensively. It was successfully used to study the saturation of the Si(100)- 2×1 surface with benzene and measure the saturation coverage.¹⁷

Figure 4 presents a comparison of SDRS spectra of a silicon surface saturated with PA or atomic hydrogen. In the case of saturation with PA, the surface received a total amount of 4.0 Langmuir which is well beyond saturation (2.9 Langmuir). The final spectra essentially display the broad peak at 2.8 eV and a shoulder at 3.8 eV. These spectra are exactly reproduced by an SDRS spectrum of a monohydride silicon surface that would be shrunk with a factor of 0.65 ± 0.03 . It is known that every

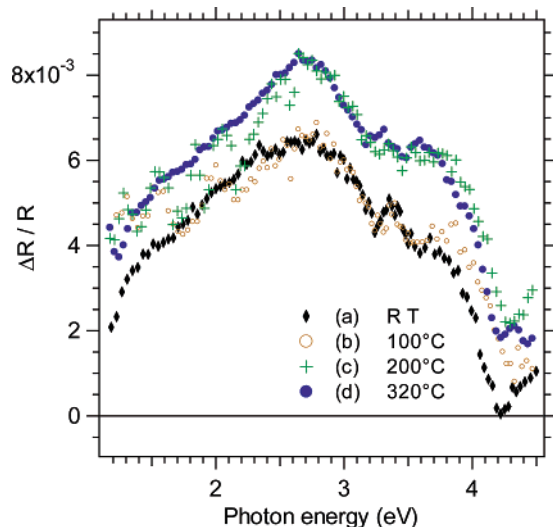


Figure 5. SDRS spectra after saturation with PA of Si(100) at different temperatures. Above 200 °C, the dissociation of PA induces a greater SDRS signal because the fragmented molecule saturates more adsorption sites of the silicon substrate.

dangling bond of a monohydride surface is saturated with one hydrogen atom; therefore in the present case, PA saturates the surface by creating a bond with $65 \pm 3\%$ of the available sites, which corresponds to a saturation coverage of $\theta = 0.65$. Moreover, none of the spectra display a strong peak at 3.8 eV that would be indicative of dimer breaking. Actually, the preservation of the dimers is confirmed by LEED images (not presented here) that show that the 2×1 reconstruction remains after deposition of PA although the image loses most of its contrast. Some of our spectra display a small peak at 3.4 eV (see 5a, 5b, and 5d) that we have disregarded because it corresponds to an ill-compensated electronic gain switching in our setup. Moreover, dissolved PA exhibits an optical absorption band at 5.0 eV,²⁵ and when PA adsorbs in an L configuration, it adopts a structure close to styrene which has an absorption band around 4.9 eV.²⁶ Actually, Spectrum 4a displays a sharp rise at 5 eV, that could be reasonably related to the optical absorption of adsorbed PA. This rise is not observed for a hydrogenated surface as presented in Figure 4b. Unfortunately, our optical setup is not sensitive enough in the 5–6 eV range to draw any stronger conclusion and analyze this optical band in detail.

Figure 5 summarizes the effect of temperature on surface coverage. Particularly, it indicates that the surface modification is identical when PA is adsorbed at room temperature and at 100 °C. This is in favor of a strong chemisorption of the molecules with no desorption pathway; otherwise, it would be thermally activated and would depend on temperature. It is likely that the impinging molecules are first physisorbed on the surface and that after some roaming about the dimers rows, they are finally strongly chemisorbed. Moreover, a saturated surface with PA cannot be recovered and if the surface undergoes a new “flash”, it results in a totally disordered surface organization. Namely, it is consistent with the dissociation observed at 320 °C, and it has been shown that the process of organic molecules breaking apart can be used to form many defects on hot silicon surfaces²⁷ and destroy them.

With SDRS, we also investigated the surface final coverage achieved by depositing PA on clean reconstructed silicon at temperatures higher than 100 °C. Spectra taken at 200 and 320 °C are identical pointing to similar final adsorption states (Figures 5c and d). The final coverage calculated by comparison

to the monohydride surface reaches $84 \pm 3\%$ of the available adsorption sites, and once again, this number does not depend on temperature. The absence of any strong peak at 3.8 eV confirms that the dimers are still intact. These optical data are consistent with the STM observation since breaking of PA into smaller species is expected to saturate more adsorption sites and yield a higher surface coverage.

To summarize these experimental data, we want to highlight the following results about the adsorption of PA on Si(100)- 2×1 :

(1) At the beginning of the adsorption process and at both room temperature and 100 °C, PA adsorbs with two configurations denoted L and S as depicted in Figure 1b. In this case, 45% of molecules are found in configuration L and 55% are found in the other one.

(2) The final surface coverage is $\theta = 0.65 \pm 0.03$.

(3) With the surface temperature set at 200 and 320 °C, adsorption leads to dissociation of PA and a total coverage of $\theta = 0.84 \pm 0.03$.

(4) The dimer reconstruction is maintained at all these investigated temperatures.

IV. Discussion

With the two surface analysis techniques we have used so far, STM and SDRS, we have access both to local information on single molecules and to global information on the covered surface. We are going to draw a more precise picture of the adsorption mechanism of PA and propose a detailed kinetic model. In particular, we want to investigate the final organization of the saturated surface.

1. Coverage as a Function of Dose: $\theta = f(x)$. Let θ be the coverage defined by the ratio per unit area of the occupied sites to the number of available sites. In the present case, an adsorption site is one silicon dangling bond. Not many techniques are able to monitor in situ the evolution of the coverage rate. In UHV, this is sometimes achieved with Auger spectroscopy or by XPS,²⁸ but it is difficult to handle. Surface differential reflectance spectroscopy is an original way to reach this same goal. The SDRS data are actually a collection of spectra recorded every two seconds during the whole adsorption process. We have so far presented spectra at saturation only. But, the remaining spectra contain valuable information about the kinetics of the process. In the case of atomic hydrogen, the number of occupied dangling bonds is proportional to the intensity of the SDRS spectrum at 2.8 eV and we have already established that saturation corresponds to a coverage of 0.65. Therefore, it is easy to extract from the set of SDRS data the evolution of θ as a function of exposure denoted x in this paper. The resulting evolution is represented in Figure 6 for various temperatures. This plot gives access to the kinetics of the reaction. With these processed data, we are now equipped to build up a simple kinetic model.

At room temperature as well as at 100 °C, the evolutions are identical and do not follow a Langmuirian process: it is impossible to fit any of these two spectra (6a and b) with an exponential curve. The corresponding Langmuirian evolution is given in Spectrum 6e, and clearly, it does not fit to the experimental data. The experimental evolution is largely linear and bends toward its horizontal asymptote very close to saturation. This almost linear coverage rate indicates that the PA sticking probability is not simply proportional to the available sites and that chemisorption is preceded by a physisorption step. The existence of a physisorbed state is confirmed by results published elsewhere for this same system where

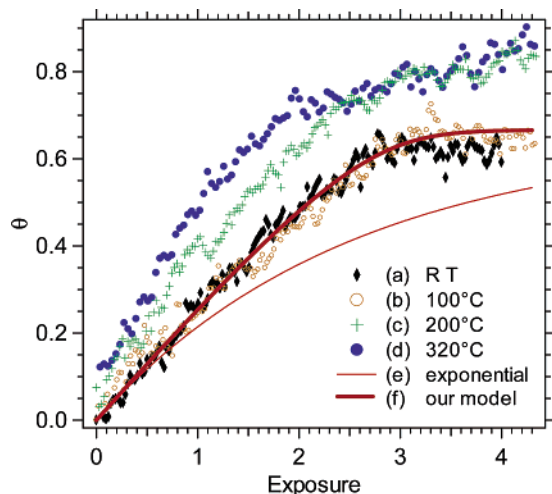


Figure 6. Evolution of the Si(100)-2 × 1 surface coverage as a function of exposure to PA for different temperatures. Coverage is calculated from the SDRS spectra. The thin solid line (e) is an exponential curve describing an adsorption obeying a Langmuirian process. The thick solid line (f) corresponds to the kinetic model developed in the text. Exposure is directly calculated from the N₂ calibrated ionization gauge.

HREELS is used to evidence a stable physisorbed layer formed at 110 K that vanishes at room temperature.¹³ This is the classical case of nonactivated physisorption where the physisorbed precursor is mobile on the surface.

2. Kinetic Model. Phenylacetylene molecules impinging on the silicon surfaces are first trapped into a physisorbed state or precursor state. Several scenarios may follow: desorption back to the gas, chemisorption, or diffusion on the surface. This is expressed by the corresponding coefficient rates which include the energies given by an Arrhenius relationship:

$$k_d = k'_d e^{-E_d/kT} \quad (1)$$

is the desorption rate and E_d is the physisorption energy of the precursor;

$$k_c = k'_c e^{-E_a/kT} \quad (2)$$

is the chemisorption rate and E_a is the activation energy representing the potential barrier that the precursor has to cross to reach the chemisorbed state.

Let N^* be the number of precursors on the surface per unit area at a given moment, and N , the number of chemisorbed species. Here, n_0 is the number of sites per unit area (number of dangling bonds). Note that the coefficients k_c and k_d can also be regarded as probabilities for chemisorption or desorption of the precursor. Consequently, the number of molecules that desorb back to gas per unit time and unit area is equal to $k_d N^*$. The number of molecules that are chemisorbed should in addition take into account that the number of available sites on the surface is not infinite (in contrast to what happens with desorption back to gas). This is expressed by a function $f_c(\theta)$ which is the probability that a molecule find an accessible site when the coverage of the surface is already θ . Therefore, $k_c N^* f_c(\theta)$ is the number of chemisorbing molecules per unit time and unit area. The f_c function strongly depends on the detailed adsorption mechanism, and we will focus on it in the next section with a Monte Carlo model. For example, with a simple adsorption geometry, such as atomic hydrogen on silicon, $f_c(\theta)$ would be $1 - \theta$.

To put into equations the evolution of the number of adsorbed molecules, we follow the classical method of the balance

equations (see, for example, refs 29 and 30). However, similar kinetic problems have been treated following the Kisliuk approach that is based on a systematic probabilistic analysis of the behaviors that a given molecule can follow on a surface. This approach conveniently explains situations where a molecule adsorbs on a given site in one given configuration^{31,32} or even when it dissociates and occupies two determined sites.^{33–35} However, for a molecule that adopts several adsorption scenarios, this approach is not suitable.

In our case, the balance equation for N^* expresses that the increase with time of the number of precursors is caused by the flux of incoming molecules (denoted Φ) and diminished by the molecules that desorb or chemisorb.

$$\frac{dN^*}{dt} = \Phi S_p f_p(N^*) - k_d N^* - k_c N^* f_c(\theta) \quad (3)$$

S_p is the sticking coefficient for the precursor and $f_p(N^*)$ is the probability that an impinging molecule finds an available site to get physisorbed.

For the chemisorbed species, the evolution equation is

$$\frac{dN}{dt} = k_c N^* f_c(\theta) \quad (4)$$

Since the chemisorbed molecule is irreversibly bound, this equation does not have any decay terms. Notice that diffusion is a process that does not affect the numbers N and N^* , so that it does not appear as an additional term in this system of equations.

To solve this differential system of equations, we assume that the number of precursors remains negligible and does not fluctuate significantly in time, so that $dN^*/dt \approx 0$. From eq 3, we have

$$N^* = \frac{\Phi S_p f_p(N^*)}{k_d + k_c f_c(\theta)}$$

And, the evolution of the chemisorbed species is obtained from eq 4:

$$\frac{dN}{dt} = \Phi S_p f_p(N^*) \frac{k_c f_c(\theta)}{k_d + k_c f_c(\theta)} \quad (5)$$

Let us now stress a delicate aspect. The adsorption of one phenylacetylene molecule occupies more than one site. Actually, the average number of sites occupied by one molecule is between two and three, depending on the adsorption geometry as revealed by STM (Figure 1b). Let α be this average number of occupied dangling bonds per adsorbed molecule. It is not a quantity easily predictable, and it will be determined in the next section with the help of the Monte Carlo model. Therefore, the surface coverage is related to the number of chemisorbed molecules by

$$\theta = \frac{\alpha N}{n_0}$$

Consequently, eq 5 becomes, after multiplication by α/n_0 ,

$$\frac{d\theta}{dt} = \frac{\alpha}{n_0} \Phi S_p f_p(N^*) \frac{k_c f_c(\theta)}{k_d + k_c f_c(\theta)} \quad (6)$$

We assume that the function f_p remains close to unity. This is justified as long as the population of precursors remains

moderate so that the impinging molecules can always find a place when landing on the surface. Equation 6 can be rewritten:

$$\frac{d\theta}{dt} \approx \frac{\alpha \Phi S_p}{n_0} \frac{f_c(\theta)}{K + f_c(\theta)} \quad (7)$$

$$\text{with } K = \frac{k_d}{k_c} = \frac{k'_d}{k'_c} e^{(E_a - E_d)/kT} \quad (8)$$

Finally, for a gas whose partial pressure is p (expressed in pascal), the corresponding dose, x , expressed in Langmuir is linked to time t by

$$dx = \frac{p}{1.23 \times 10^{-4}} dt$$

and the total flux of impinging molecules of mass m is given by the kinetic theory of gases:

$$\Phi = \frac{p}{\sqrt{2\pi mkT}} \quad (9)$$

So that, the final form of the evolution equation of the coverage is

$$\frac{d\theta}{dx} = \frac{\alpha \times S_p \times 1.23 \times 10^{-4}}{n_0 \sqrt{2\pi mkT}} \frac{f_c(\theta)}{K + f_c(\theta)} = A \frac{f_c(\theta)}{K + f_c(\theta)} \quad (10)$$

A is a coefficient that could be evaluated numerically if we had access to the actual exposure x which is not the case with our experimental setup, as explained in section II. Notice that $d\theta/dx$ is the sticking coefficient, often defined by $S(\theta)$. This latter equation can now be checked against the data provided that an expression is given to the function f_c . This is the scope of the following section.

3. Monte Carlo Calculations To Evaluate the f_c Function.

The function $f_c(\theta)$ is the probability that a precursor finds an available site for adsorption. The intricate aspect with phenylacetylene, is that this molecule may adopt two very different adsorption configurations as evidenced by the STM results presented in section III. Phenylacetylene dimensions are given in Figure 1a and, it is worth noting that the molecule could be accommodated on the surface in tight configuration: its length perfectly matches the dimer spacing of the reconstructed surfaces. In the L configuration, PA attaches to two adjacent dangling bonds (see Figure 7a). But, the phenyl ring partially blocks the access to the adjacent dangling bond as it appears in Figure 7b which shows an example of a 10×5 dimers surface saturated with PA. If a PA molecule adsorbs with its phenyl tail oriented to the right, the nearest neighbor dimer can accommodate another molecule in an L configuration only if this one adopts the same orientation: phenyl tail to the right. This is the case of the first line of Figure 7b for the couple of L molecules marked with an arrow. Notice that entire dimers may be totally blocked toward further adsorption even if none of its dangling bond are touched by a molecule as it occurs on the sixth dimer line of Figure 7b. The S configuration occupies three dangling bonds of three different dimers. The phenyl binds to two dangling bonds of two adjacent dimers as represented in Figure 7a and loses its electronic conjugation in the operation. This phenyl group partially blocks the other two dangling bonds and prevents large groups from binding to these sites.

A Monte Carlo model has been designed consequently. At every step, a dangling bond is randomly chosen, and if this site

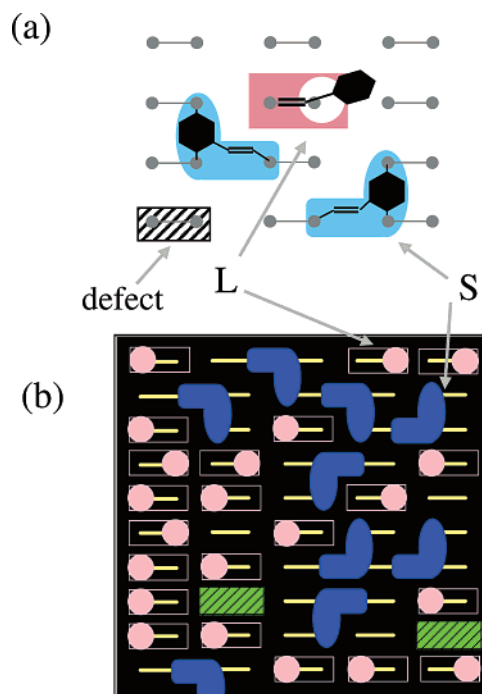


Figure 7. (a) Monte Carlo model of adsorption of PA on the silicon dimers taking into account the two possible adsorbed species L and S. (b) Partial view of a saturated silicon surface as calculated with our Monte Carlo model. The surface is modeled with 100×100 silicon atoms with 3% defects.

is free, an adsorption configuration is tossed according to the initial sticking probabilities observed with STM: 45% for L and 55% for S. Next, the program checks if the molecule has enough room to accommodate around that dangling bond in the chosen configuration. Figure 7b is a zoom-in of a typical result after saturation of a 100×100 atoms surface. To reproduce more precisely the STM facts, defects have been considered: two of them are visible in Figure 7b. This final saturated surface exhibits a quite large number of unoccupied dangling bonds (32%). It is easy to check that none of the L or S species can fit in these empty spots.

This Monte Carlo code has been programmed with the software Igor Pro (WAVEMETRICS Inc.) that offers an efficient C compiler and a handful ways to visualize the progress of molecular adsorption. The code returns the evolution of the total coverage θ according to its definition given in the previous section as well as the ratio of the L and S successfully adsorbed species. The final coverage does not depend on the size of the chosen surface provided that it contains more than 800 dimers. In other words, irregular adsorption configurations occurring on the edges of the computed surfaces become negligible over 800 dimers. Figure 8 presents the result of a run for a surface with 100×100 silicon atoms (5000 dimers) and 3% randomly distributed defects. Saturation is achieved after having thrown 120 000 molecules on the surface. This calculation returns a final total coverage of 0.650 ± 0.005 , that exactly matches the measurements made with surface differential reflectance spectroscopy which were presented in section III-2. The model easily allows exploring the behavior of the system when changing some parameters. For example, if all the molecules had been adsorbing in an L configuration, the final coverage would be 0.78 and, in the case of the S configuration, it would be 0.50. Therefore, the final coverage really expresses a balance between L and S species adsorbed on the surface. The tight correspondence between model and experiments is a strong support of the coherence between STM observations, optical measure-

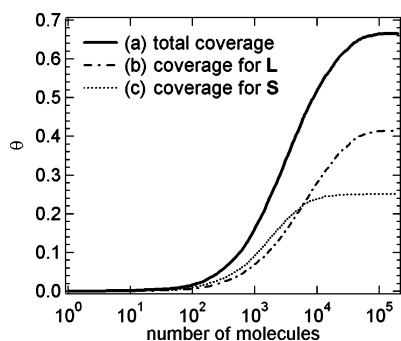


Figure 8. Evolution of the total coverage (a) and partial coverages for L species (b) and S species (c) predicted by our Monte Carlo model. This calculation is performed for silicon surfaces with 100×100 silicon atoms with 3% defects and initial sticking probabilities of 45% and 55% for L and S, respectively.

ment, and Monte Carlo simulation, so that the final molecular organization calculated by our model is trustworthy.

Moreover we have access to the partial coverages of L and S species denoted respectively $\theta_L(\theta)$ and $\theta_S(\theta)$. Figure 8 shows that, at the beginning, S species are filling up the dangling bonds more rapidly, which is a consequence of their higher initial sticking probability (55%) and illustrates the fact that they need three dangling bonds to accommodate. But around a coverage of 0.23, the S species loses ground before the L adsorption configuration, and from this point on, the adsorption is highly competitive between the two species. From these partial coverages, we calculate that, at saturation, the population has a composition reversed compared to the initial trend: 71% of the adsorbed species are of type L, and 29% are of type S.

Above all, the probability of an incident molecule to find an accessible site can be extracted from these simulations. This is the f_c function, mentioned in the previous paragraph, and it is given by

$$f_c(\theta) = 1 - \frac{\frac{1}{2}\theta_L(\theta) - \frac{1}{3}\theta_S(\theta)}{\frac{1}{2} \times 0.40 - \frac{1}{3} \times 0.25} = \frac{0.99 - 1.26\theta - 0.34\theta^2}{0.99 - 1.26\theta - 0.34\theta^2} \quad (11)$$

which turns out to be very close to a linear evolution with the form $f_c(\theta) \approx 1 - \theta/0.65$.

These calculations also give access to the number α defined as the average number of occupied dangling bonds per adsorbed molecule. This number almost linearly decreases from 2.5 to 2.3 sites per phenylacetylene molecule as the coverage increases. We will use the average value of 2.4 for our calculations.

Finally, the image of the completely saturated surface obtained with the model shows a highly disordered surface, with an intricate combination of L and S species and no special domain formation.

4. Comparison of the Model with the Experimental Data.

In this section, we put together all the elements discussed before and compare the model to the experimental data. Equation 10 combined with expression for the f_c function (eq 11) gives the evolution of coverage as a function of the amount of incoming molecules, provided that the differential equation is solved. This is done numerically with an Euler method. The two parameters A and K are found to have the following values: $A = 0.30 \pm 0.01 \text{ L}^{-1}$ and $K = 0.15 \pm 0.05$. These values ensure an almost perfect match between the theoretical model and experimental data as shown in Figure 6.

Parameter A is related to the initial sticking probability (see eq 10). Parameter K results from the competition between

desorption and chemisorption as shown by relation 8, and it is the only temperature-dependent parameter. Since the kinetic evolution is exactly the same for room temperature and 100 °C, this implies that there is no actual temperature dependence or that it is beyond the accuracy of our measurement. It results that the activation energy and the desorption energy are of the same order of magnitude or, to be more precise, $|E_a - E_d| < 0.5 \text{ eV}$. Finally, relation 8 becomes $k'_d \approx 0.15k'_c$, which means that a PA precursor get chemisorbed seven times more quickly than desorbed.

The absence of detectable temperature dependence in the adsorption of PA on silicon is all the more a striking result because Tao et al.¹³ pretend that at 110 K PA adsorbs with the L configuration only, whereas, at room temperature, both L and S configuration are detected on the surface. Actually in the possible configurations Tao et al. consider, they omit those implying several neighboring dimers as it is the case for our S configuration. Moreover, the HREELS spectra they show are compatible with the coexistence of the two L and S species. It is very likely that they have not considered the S adsorbed species. Therefore, their results are not an argument for a temperature dependence of PA adsorption, and probably, even at 110 K, PA also adsorbs with the two L and S configurations.

V. Conclusion

Phenylacetylene adsorption on $\text{Si}(100)\text{-}2 \times 1$ is studied from low coverage up to saturation. STM study at the molecular level reveals that PA adsorbs on the dimers following two distinct modes involving either two or three dangling bonds. The L mode appears like large and bright spot and probably owes its strong STM contrast to the wide electronic delocalization throughout the molecule. It occupies a single dimer. This is the most interesting configuration in terms of further use of this molecule in the context of molecular electronics. An appealing challenge is to cover the entire silicon surface with such species. One would expect a strong electronic effect and even an anisotropic charge transport. However, this hope is thwarted by the other possible adsorption geometry denoted S and detected with the STM as a smaller protrusion. In this scenario, PA sits on three dangling bonds and strongly blocks the adsorption of the L configuration. The coexistence of these two geometries on the surface is competitive. Our Monte Carlo program illustrates this struggle and greatly complements the information gained with STM. A patchy and disorganized surface results from the completed adsorption. Both the model and the optical measurements show that the maximum coverage is 0.65. Moreover, this model provides useful quantities that made it possible to design a kinetic model of the evolution of coverage. This theoretical evolution of coverage is compared with the experimental optical data and perfectly agrees with them. The agreement is very good especially for such a complex molecular system.

Finally, temperature seems not to be the right parameter to adjust the balance between the L and S populations. STM at initial coverage as well as SDRS at saturation record exactly the same data at the two temperatures where dissociation does not take place.

Although phenylacetylene is not a self-organizing system by direct adsorption on the clean reconstructed silicon surface, it certainly deserves further studies. It belongs to the kind of molecule that bears promises for building an ultrathin, structurally and electronically homogeneous layer that industry is battling to design and replace the Si/SiO_2 interface that is pushed to its ultimate limits.

Acknowledgment. The STM images were processed with WSxM software which is free software that is downloadable at <http://www.nanotec.es>. This work was supported by grants from Région Ile-de-France.

References and Notes

- (1) Shaw, J. M.; Seidler, P. F. *IBM J. Res. Dev.* **2001**, *45*, 3.
- (2) Hamers, R. J.; Hovis, J. S.; Lee, S.; Liu, H.; Shan, J. *J. Phys. Chem. B* **1997**, *101*, 1489.
- (3) Bent, S. F. *Surf. Sci.* **2002**, *500*, 879.
- (4) Mezheny, S.; Lyubnitsky, I.; Choyke, W. J.; Wolkow, R. A.; Yates, J. T., Jr. *Chem. Phys. Lett.* **2001**, *344*, 7.
- (5) Witkowski, N.; Pluchery, O.; Borensztein, Y. *Phys. Rev. B* **2005**, *72*, 75354.
- (6) Hofer, W. A.; Fisher, A. J.; Lopinski, G. P.; Wolkow, R. A. *Phys. Rev. B* **2001**, *63*, 085314/1.
- (7) Hofer, W. A.; Fisher, A. J.; Lopinski, G. P.; Wolkow, R. A. *Surf. Sci.* **2001**, *482–485*, 1181.
- (8) Mayne, A. J.; Lastapis, M.; Baffou, G.; Soukiassian, L.; Comtet, G.; Hellner, L.; Dujardin, G. *Phys. Rev. B* **2004**, *69* (4), 45409.
- (9) Hacker, C. A.; Hamers, R. J. *J. Phys. Chem. B* **2003**, *107*, 7689.
- (10) Hung, L. S.; Chen, C. H. *Mater. Sci. Eng., R* **2002**, *39*, 143.
- (11) Tao, F.; Wang, Z. H.; Lai, Y. H.; Xu, G. Q. *J. Am. Chem. Soc.* **2003**, *125*, 6687.
- (12) Kim, K.-Y.; Song, B.-K.; Jeong, S.; Kang, H. *J. Phys. Chem. B* **2003**, *107* (43), 11987.
- (13) Tao, F.; Qiao, M. H.; Li, Z. H.; Yang, L.; Dai, Y. J.; Huang, H. G.; Xu, G. Q. *Phys. Rev. B* **2003**, *67*, 115334.
- (14) Cicero, R. L.; Linford, M. R.; Chidsey, C. E. D. *Langmuir* **2000**, *16*, 5688.
- (15) Saito, N.; Hayashi, K.; Sugimura, H.; Takai, O. *Langmuir* **2003**, *19*, 10632.
- (16) Bartmess, J. E.; Georgiadis, R. M. *Vacuum* **1983**, *33*, 149.
- (17) Witkowski, N.; Pluchery, O.; Borensztein, Y. *Phys. Rev. B* **2005**, *72*, 75354.
- (18) Borensztein, Y.; Pluchery, O.; Witkowski, N. *Phys. Rev. Lett.* **2005**, *95*, 117402/1.
- (19) Ja-Yong, K.; Jae-Yel, Y.; Chanyong, H.; Dal-Hyun, K.; Sekyung, L.; Dong-Hyuk, S. *Phys. Rev. B* **1995**, *52*, 17269.
- (20) Ukraintsev, V. A.; Yates, J. T., Jr. *Surf. Sci.* **1996**, *346*, 31.
- (21) Hata, K.; Kimura, T.; Ozawa, S.; Shigekawa, H. *J. Vac. Sci. Technol. A* **2000**, *18*, 1933.
- (22) Kruse, P.; Wolkow, R. A. *Appl. Phys. Lett.* **2002**, *81* (23), 4422.
- (23) Borensztein, Y. *Phys. Status Solidi A* **2005**, *202*, 1313.
- (24) Borensztein, Y. *Surf. Rev. Lett.* **2000**, *7*, 399.
- (25) *The Handbook of Infrared and Raman spectra of Inorganic Compounds and Organic Salts*; Nyquist, R. A., Ed.; Academic Press: New York, 1997.
- (26) The Chemistry Webbook of the National Institute of Standards and Technology. <http://webbook.nist.gov> (accessed 2005).
- (27) Suzuki, T.; Maksymovych, P.; Levy, J.; Yates, J. T., Jr. *Surf. Sci.* **2006**, *600*, 366.
- (28) Joseph, Y.; Kuhrs, C.; Ranke, W.; Ritter, M.; Weiss, W. *Chem. Phys. Lett.* **1999**, *314*, 195.
- (29) Dwyer, D. J.; Simmons, G. W.; Wei, R. P. *Surf. Sci.* **1977**, *64*, 617.
- (30) Takaoka, T.; Kusunoki, I. *Surf. Sci.* **1998**, *412–413*, 30.
- (31) Kisliuk, P. *J. Phys. Chem. Solids* **1957**, *3*, 95.
- (32) Witkowski, N.; Coustel, R.; Pluchery, O.; Borensztein, Y. *Surf. Sci.*, in press.
- (33) Kisliuk, P. *J. Phys. Chem. Solids* **1958**, *5*, 78.
- (34) Ranke, W.; Xing, Y. R. *Surf. Sci.* **1997**, *381*, 1.
- (35) Ranke, W. *Surf. Sci.* **1996**, *369*, 137.